BNL-220732-2020-TECH
EIC-HDR-TN-015

Design of electron storage ring for high-energy EIC cooling

J. Kewisch

December 2020

Electron-Ion Collider

Brookhaven National Laboratory

U.S. Department of Energy

USDOE Office of Science (SC), Nuclear Physics (NP) (SC-26)

DISCLAIMER

EIC TECHNICAL NOTE	NUMBER **EIC-HDR-TN-015**
AUTHORS: J. Kewisch, He Zhao, M. Blaskiewicz, A. Fedotov	DATE 12/21/2020
Design of electron storage ring for high-energy EIC cooling	

December 21, 2020

Design of electron storage ring for high-energy EIC cooling

J. Kewisch, He Zhao, M. Blaskiewicz, A. Fedotov

1 Abstract

We present a possible layout for an the Electron-Ion Collider electron cooler based on a storage ring which employs a wiggler section for the cooling of the electrons through radiation damping. We describe the optics, first and second order chromaticity correction and calculate the dynamic aperture. Finally, we estimate the damping times of the ion in EIC.

2 Introduction

In order to reach the highest luminosities in the BNL Electron-Ion collider (EIC) cooling of the ions is considered. Besides nouvelle variants of stochastic cooling like micro-bunched electron cooling and coherent electron cooling the classical electron cooling is a candidate.
Since the required electron energy is above what can be achieved with an un-bunched beam the typical approach is to use a super-conducting energy recovery linac. The biggest problem with this approach is the need for an electron gun capable of delivering a sufficiently high beam current and cathode lifetime.
One way to overcome this obstacle is using a storage ring for the electrons, so that they don't have to be replaced continuously. This approach is not new and has been discussed before [1, 2, 4, 5]. In this scenario the electrons will cool the ions and are cooled themselves by radiation damping, which is enhanced by wiggler magnets.
The feasibility of this approach is in the details: The wiggler section will create a large chromaticity due to the weak focusing of the dipoles. Since the arcs are relatively small there are only a few slots available to place sextupoles, and the dispersion has to be kept small to avoid a transverse emittance growth from intra-beam scattering. Therefore the sextupoles have to be strong which decreases dynamic aperture.
The only other place for sextupoles is inside the wiggler magnets, where a small dispersion can be available throughout the length of the magnet, requiring smaller sextupole field strength. Also, since wigglers focus the beam in one plane, but don't defocus in the other plane, a large ratio between horizontal

and vertical beta functions can be maintained, making the chromaticity compensation more effective. In our setup the ratio of the beta functions is about 100.
Still, the increase of the transverse emittance, which is proportional to $H = \gamma D^2 + 2\alpha D D' + \beta D'^2$ must be minimized. Since the D'^2 term of the H function is two orders of magnitude bigger than the other terms, the dispersion in the wiggler section does not have to be small, as long as D' is kept small.

3 The Wiggler section

In our setup we use alternating horizontal and vertical wigglers. Each wiggler is 7.44 meters long. The poles are shaped as combined function sector dipoles, where the gradient is $k = \rho^{-2}$. This transfers the weak focusing from the wiggler plane into the perpendicular plane, where the beta function is matched to be equal to the bend radius and therefore is constant. In the wiggler plane the beta function is chosen to be 25 m. With no focusing in the wiggler plane D' stays zero throughout the wiggler.

Magnetic Field	1.88 T
Length	7.44 m
Bending Radius	0.2461 m
Number of poles	158
Wiggler period	4.8 cm
Beta function in the wiggle plane	25 m
Beta function perpendicular	0.2461 m
Dispersion	75 cm
Number of wiggler magnets	16
Sextupole pole tip field at 2 cm	177 G

Tab. 1: Wiggler parameters

Alternatively, one could use rectangular wiggler poles to transfers the weak focusing from one plane to the other. However, the weak focusing in the middle of the poles in compensated at the ends, and the difference in location causes D' to be non-zero and proportional to the value of D. This causes a significant increase of the emittance.
On each side of the wigglers are two dipoles that create a step in the beam line and thus create dispersion. Using quadrupoles the dispersion is then amplified to the desired value and D' is made zero at the entrance of the wiggler.

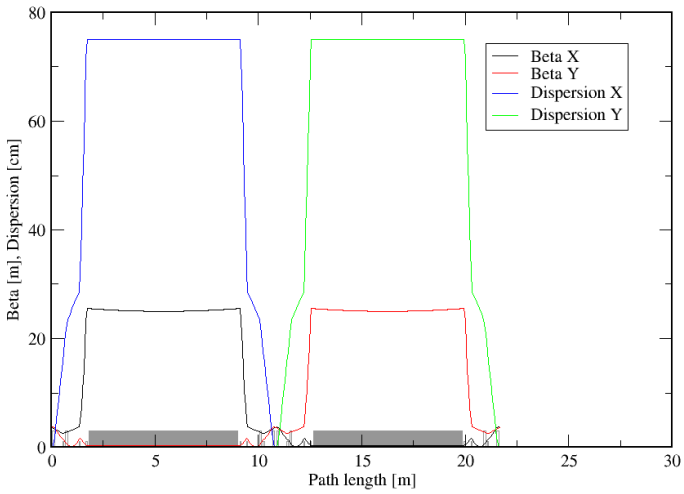

Fig. 1: Twiss functions in the wiggler.

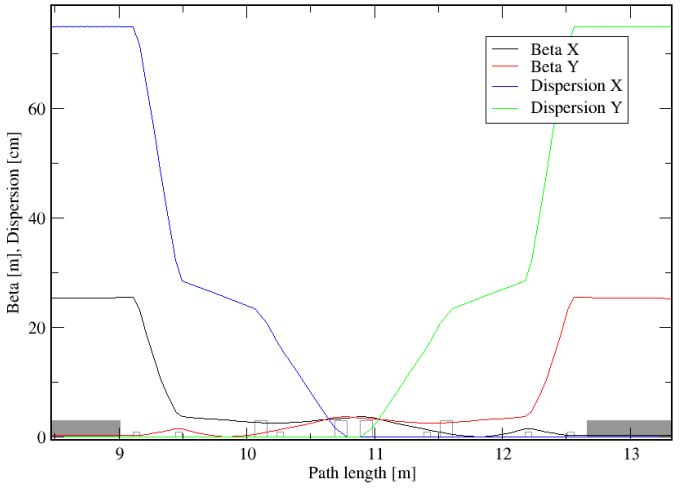

Fig. 2: Twiss functions in the transition between wigglers

We evaluated different values for the dispersion and settled on 75 cm. A smaller

dispersion gives a better beam emittance, but requires stronger sextupoles. A larger dispersion increases the IBS contribution outside the wigglers and creates a significant shift of the closed orbit at larger momentum deviations, which reduces the dynamic aperture. We have not performed a careful scan of the dispersion to find the optimum value.
The ring has a 2-fold mirror symmetry, and each half has four pairs (horizontal and vertical) wigglers. By selecting the fractional part of the phase advance over a wiggler pair to be 1/4th or 3/4th any focusing kicks caused by sextupole components are compensated in the next pair, any orbit kicks are compensated in the second next pair.
This phase advance is dominated by the beta function in the non-wiggle plane, which we chose to be the bend radius. To fulfill the above condition we have to select discrete wiggler field strength.
We used the GETRAD program to find the optimum field strength. This program finds for a given optics the equilibrium emittances and energy spread considering quantum excitation, intra-beam scattering, ion-heating and radiation damping.
The results for the nominal bunch charges of $3 \cdot 10^{11}$ are shown in figures 3, 4 and 5.
The best cooling rate is achieved with high wiggler field strength. However, a stronger filed quadratically increases the weak focusing, which increases the chromaticity, which requires stronger sextupoles and reduces the dynamic aperture. Also the difficulty of engineering the wigglers increases with higher field. We settled on a compromise with a field strength of 1.88 T. The improvement of the cooling time with higher wiggler field above this point is only gradual and does not warrant the technical difficulties.

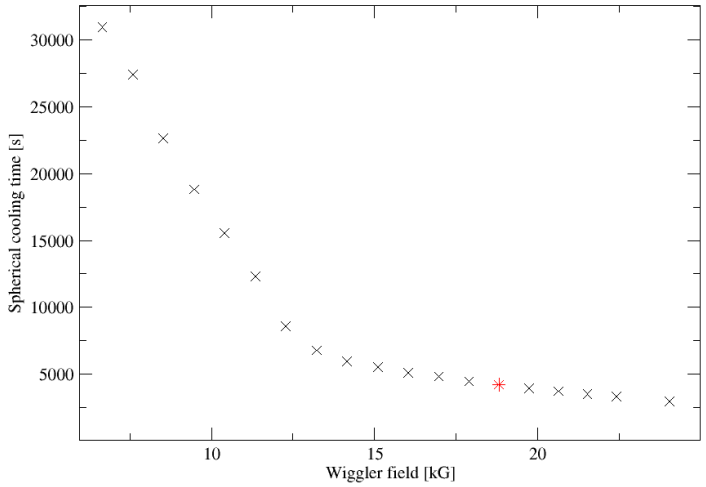

Fig. 3: Spherical cooling time as function of the wiggler field. The selected working point is indicated by the star.

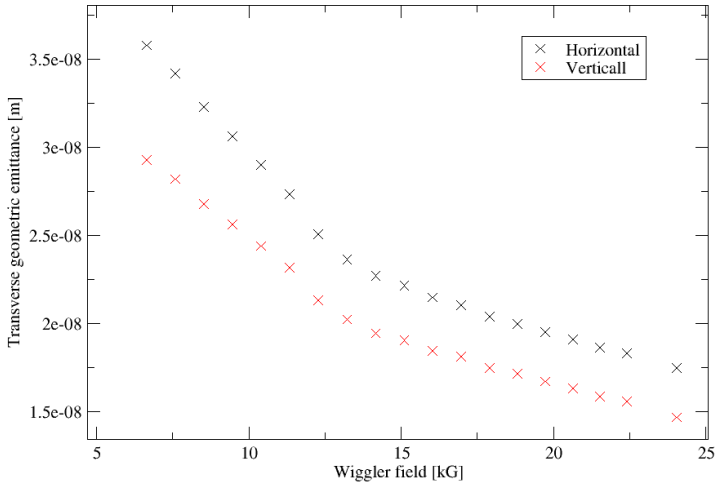

Fig. 4: Geometric emittance as function of the wiggler field.

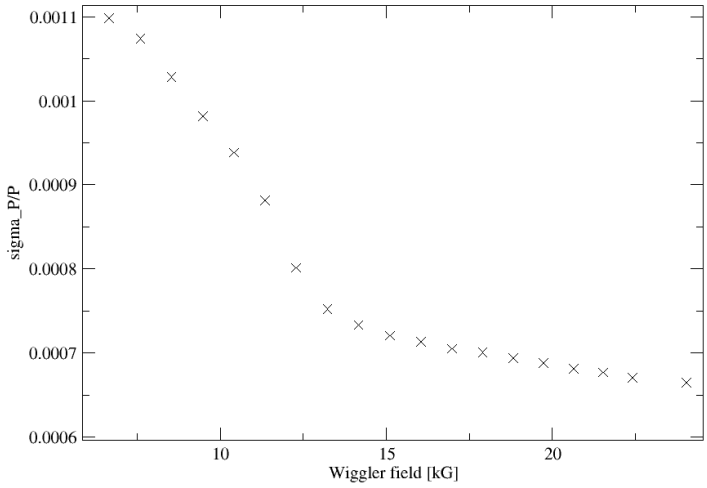

Fig. 5: RMS energy spread as function of the wiggler field

4 The storage ring

The ring has a race track shape, where the cooling section is in one straight section and the wigglers are in the other. It is mirror symmetric around the center of the cooling section.
Figure 6 shows the top view of the complete accelerator. The cooling section has a length of 170 meters, so that it fits into one of the straight sections of RHIC.
There are four 90^o arcs with a radius of 3.42 meters. Each arc has 10 dipoles and a 90 degree phase advance per cell. The maximum dispersion is 16.3 cm.
Since the electron beam has a too high energy to be turned around inside RHIC tunnel the mid-arc adapters take the beams through the tunnel walls into a separate building for the wiggler section. The mid-arc adapters are also used to adjust the tunes of the machine.
The wiggler section is mirror-symmetric with four pairs of wigglers in each half. The mid-wiggler adapter connects the two parts, but is also used to optimize the higher order chromaticity, which is essential for obtaining a sufficient dynamic aperture.
Instead of using multiple sextupole families we adjust the phase advance in the mid-wiggler adapter so that the driving terms [3] of the first half of the machine cancel the terms of the second half, using the mirror symmetry of the ring.

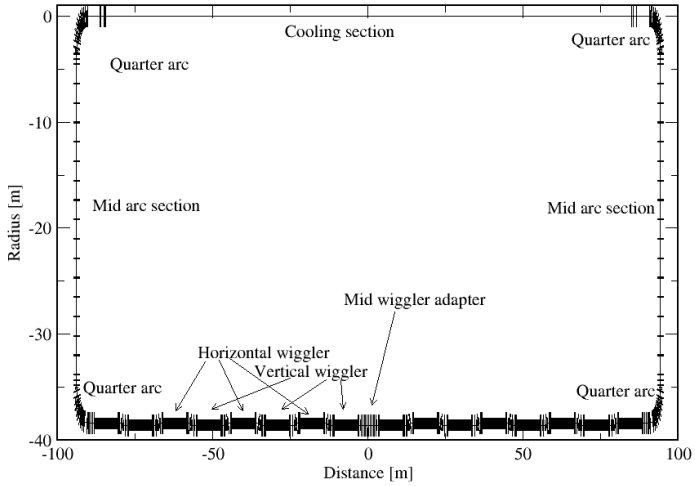

Fig. 6: Layout of the cooler. The mid-arc adapter and mid-wiggler adapter are quadrupole sections, allowing to adjust the phase advance to set the tunes and minimize the beta beat of the machine.

Table 3 has the relevant parameters for cooling 275 GeV protons.

Parameter	value
Circumference	449.08 m
Length of cooling section	170 m
Lorentz factor γ	293.093
Beam energy	149.26 MeV
Energy loss per turn U_0	270 eV
Arc radius	3.42 m
Number of arc dipoles	40
arc dipole field	3.64 kG
Dispersion in arc	18.5 cm
Electrons per bunch	3×10^{11}
Peak current	38.5 A

Tab. 2: Storage ring parameters

Parameter	value
Horizontal tune	59.848
Vertical tune	59.917
Natural horizontal Chromaticity	-117.8
Natural vertical Chromaticity	-114.4
Momentum compaction	$-3.21 \cdot 10^{-3}$
Horizontal damping constant	31.5 s^{-1}
Vertical damping constant	31.4 s^{-1}
Longitudinal damping constant	63.6 s^{-1}
Horizontal damping time	0.03173 s
Vertical damping time	0.03178 s
Longitudinal damping time	0.01571 s
RMS bunch length	10cm
Horizontal emittance excluding IBS and ion heating	$3.07 \cdot 10^{-9}$ m
Vertical emittance excluding IBS and ion heating	$3.11 \cdot 10^{-9}$ m
Horizontal emittance including IBS and ion heating	$2.1 \cdot 10^{-8}$ m
Vertical emittance including IBS and ion heating	$1.8 \cdot 10^{-8}$ m
β_x in the center of the cooling section	153.7 m
β_y in the center of the cooling section	273.6 m
Horizontal RMS beam radius ion the cooling section	1.75 mm
Vertical RMS beam radius ion the cooling section	2.44 mm

Tab. 3: Storage ring optical parameters

5 Optics matching

The Twiss functions of the ring are shown in figure 7. It is desirable to have a large beta function in the cooling section, so that the transverse temperature of the electrons are minimized. However, if the beta functions are equal in horizontal and vertical direction and quadrupoles are used to focus the beam into the arc structure then one of the directions must be defocused before both functions can be matched to the arc values. This leads to unacceptably large beta functions ($\tilde{6}$00 m) and a significant contribution to the chromaticity.

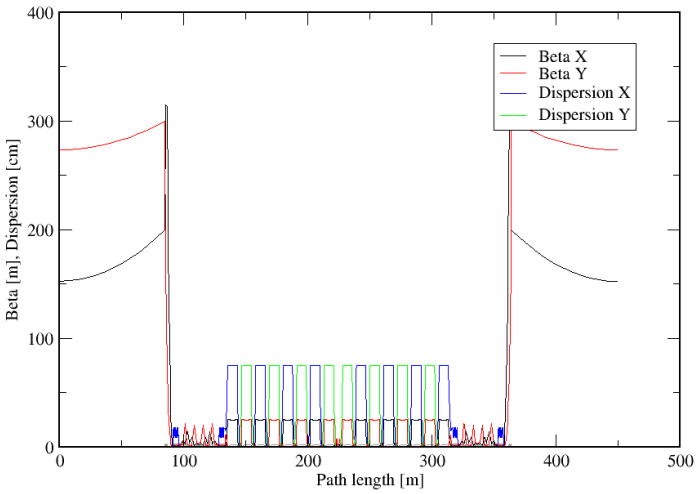

Fig. 7: Optical functions of the ring, The start point is the center of the cooling section.

In our design we use therefore unequal beta functions: $\beta_x = 152.7$ m, $\beta_y = 273.6$ m in the center of the cooling section. With this arrangement the peak beta function does not exceed 315 m, as shown in figure 8.
As mentioned before the slope of the dispersion is the major contribution to IBS. At the transition from the arc to the wiggler section the arc dispersion is not matched to zero, but is raised to match the dispersion required in the wiggler (figure 9).

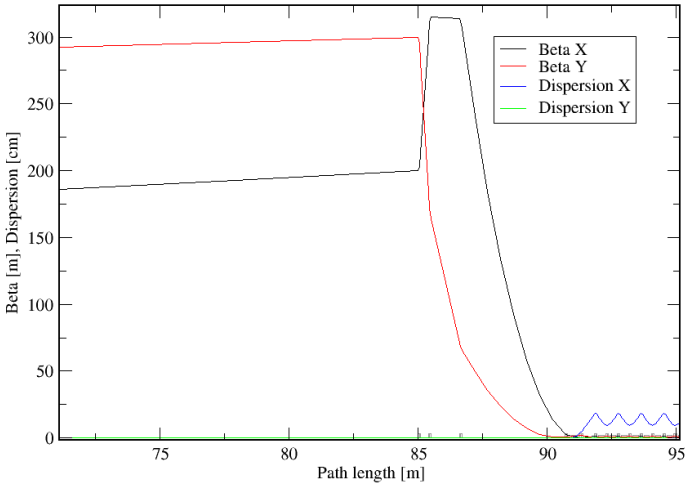

Fig. 8: Optical functions of the ring, zoomed into the transition from the cooling section to the arc.

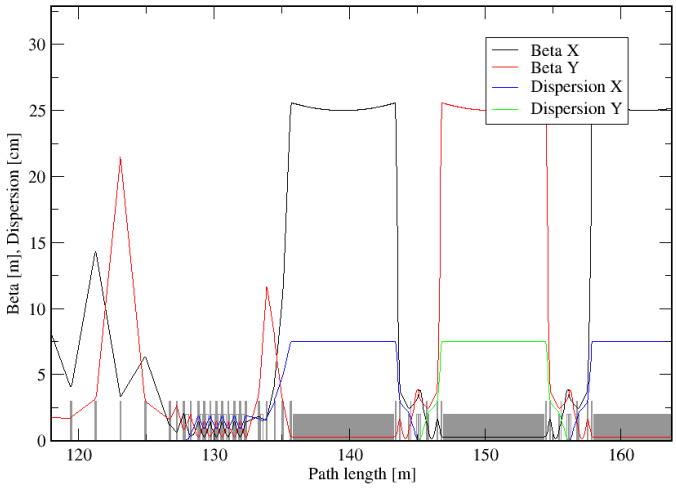

Fig. 9: Optical functions of the ring, zoomed into the transition from the cooling section to the arc.

For the longitudinal dynamic aperture the non-linear behavior of the machine was minimized manually by changing the sextupole strength and the phase advance across the mid-arc and mid-wiggler adapters. For that purpose we tracked particles at fixed momentum offset (RF cavities turned off) using the ELEGANT program [6]. For comparison the tracking was also done using the PTC function of the MADX program, giving the same results. The tunes were obtained from an FFT of the turn-by-turn data, the closed orbit is the average of this data, and the beta function comes from:

$$\epsilon = \sqrt{\sum x^2 \sum x'^2 - \left(\sum xx'\right)^2} \tag{1}$$

$$\beta = \frac{\left(\sum x^2\right)}{\epsilon} \tag{2}$$

Because the space charge tune shift reduces the tune of the machine we chose a tune just below the integer. We found that when the fractional phase advance across a pair of wigglers is 1/4th the machine tune for large momentum deviation is lower, for 3/4th it is higher. We settled on a phase advance of 6.25, close to the minimum of the spherical cooling time.

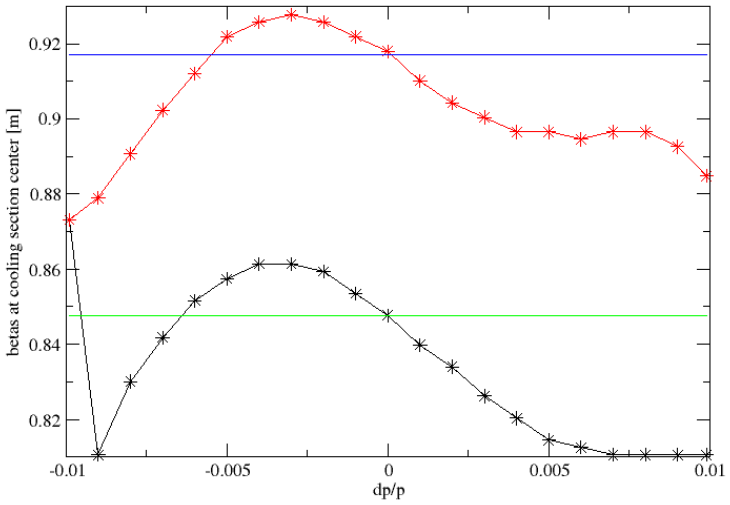

Fig. 10: Tunes as function of constant energy deviation

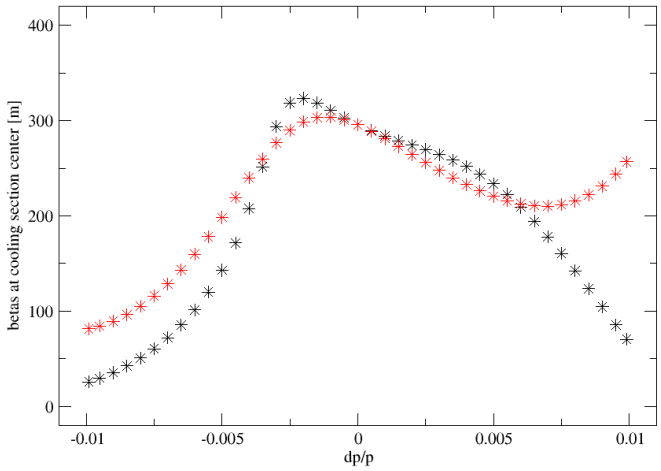

Fig. 11: Beta function vs constant energy deviation

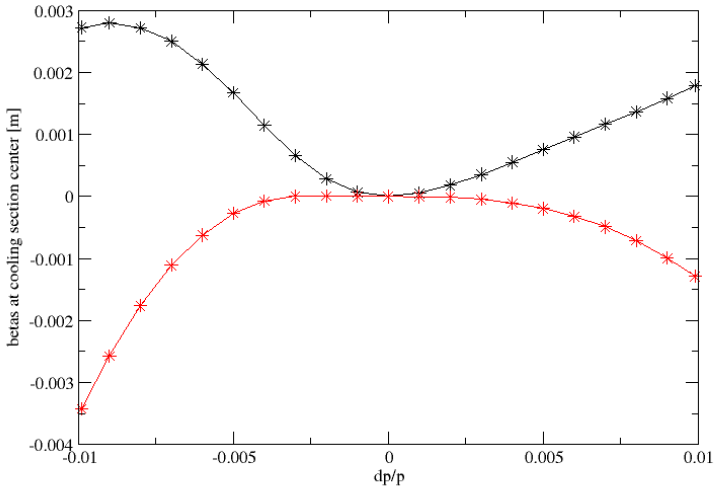

Fig. 12: Orbit in the center of the cooling section as function of constant energy deviation. Because of the ring symmetry the slope of the orbit is zero at this location.

The first goal of the optimization was not to cross the resonance lines at -1/4th and -1/3rd. At the same time we have to watch the off-energy closed orbit. Large orbit deviations will reduce the dynamic aperture. Finally, the curve of the beta functions gives information about the expected dynamic aperture. We see in this case that for large negative momentum deviations the beta functions become small in the center of the cooling section, which means they will be large elsewhere. There is room for improvement.

6 Dynamic aperture

We then test the dynamic aperture with particle tracking using ELEGANT. In this calculation we included an RF cavity. The voltage is set to produce a 10 cm RMS bunch length. The results are shown in Figures 13 and 14, where the initial radius and momentum deviation of electrons that survived 1000 ($\approx$ one damping time) turns is plotted in black, the ones that got lost are in red. The axis are in units of sigmas, which is obtained from the GETRAD program.

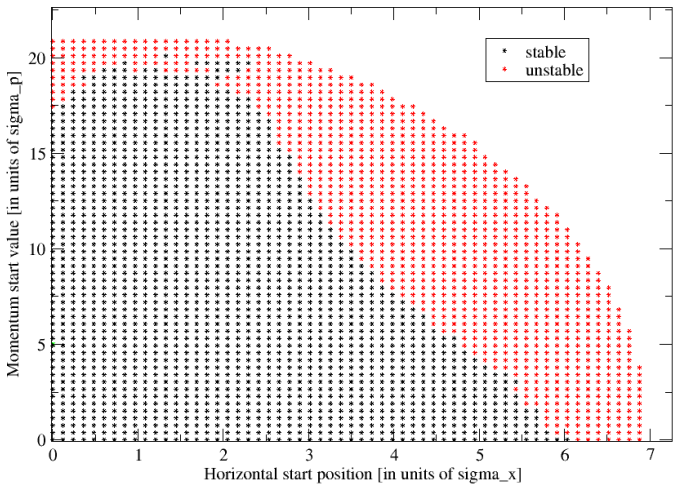

Fig. 13: Dynamic aperture.

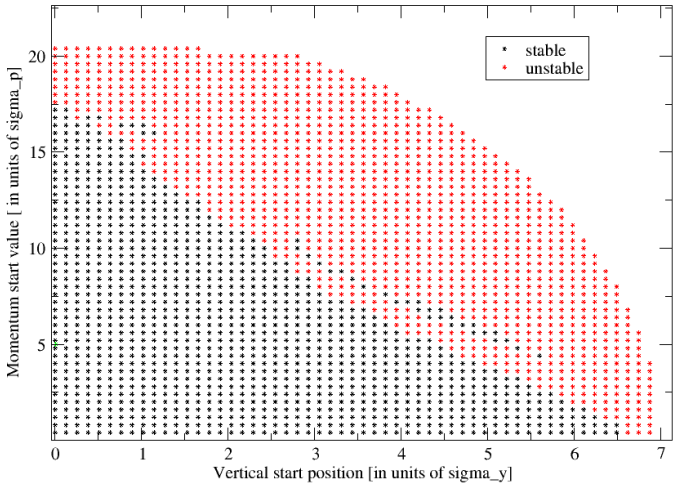

Fig. 14: Dynamic aperture.

We find a dynamic aperture of 6.3 sigmas in horizontal direction, 6.5 in vertical and 17.5 in longitudinal direction. The beam life time is given by Piwinski's formula [8]:

$$\frac{1}{\tau} = 2\alpha_\beta r_\beta \exp\left(-r_\beta\right) \tag{3}$$

where α_β is the damping constant and

$$r_{beta} = \frac{1}{2}\left(\frac{x_{da}}{\sigma_x}\right)^2 \tag{4}$$

with x_{da} being the dynamic aperture. Inserting the parameters gives $3 \cdot 10^6$ seconds, infinite for all practical purposes.

7 Conclusion

Detailed design of electron cooler storage ring is presented. By moving the sextupoles inside the wiggler magnets we opened a path for using a storage ring cooler for the EIC. A cooling time of about one hour [9] might provide sufficient cooling for the protons at the top energy of 275 GeV in the EIC and provide a low cost alternative to other cooling schemes.

References

[1] D. Cline et al., "High energy electron cooling to improve the luminosity and lifetime in colliding beam mahines", in Proc. of Particle Accelerator Conference 1979, IEEE Transactions of Nuclear Science, Vol. NS-26, No. 3 (1979).

[2] M. Gentner, R. Brinkmann, Ya. Derbenev, D. Husmann, C. Steier, "On the possibilities of electron cooling for HERA", NIMA vol 424, p 277-295 (1999).

[3] Y. Luo, S. Tepikian, W. Fischer, G. Robert-Demolaize, D. Trbojevic: "Sorting Chromatic Sextupoles for Second Order Chromaticity Correction in the RHIC", Proceedings of IPAC'10, Kyoto, Japan

[4] P. Wesolowski, K. Balewski, R. Brinkmann, K. Floettmann, Ya. Derbenev, Yu. Martirosian: "Electron Cooling At PETRA using a Bunched Beam"

[5] A. Burov, V. Danilov, P. Colestock, Ya. Derbenev, "Electron cooling for RHIC", NIMA Vol 441, p 271-273 (2000)

[6] M. Borland, "elegant: A Flexible SDDS-Compliant Code for Accelerator Simulation," Advanced Photon Source LS-287, September 2000.

[7] F. Schmidt, "MAD-X PTC INTEGRATION", Proceedings of 2005 Particle Accelerator Conference, Knoxville, Tennessee

[8] A. Piwinski, "BEAM LOSSES AND LIFETIME", CERN accelerator school.

[9] H. Zhao, J. Kewisch, M. Blaskiewicz, A. Fedotov, "Ring-based electron cooler for EIC", BNL-220731-2020-TECH (December 2020).